Journal of Thermal Analysis, Vol. 51 (1998) 91-104

THE BEHAVIOUR OF WATER MOLECULES ASSOCIATED WITH STRUCTURAL CHANGES IN NEGATIVELY CHARGED PHOSPHATIDYL-GLYCEROL ASSEMBLIES AS STUDIED BY DSC

M. Kodama, Junji Nakamura, Takahiro Miyata and Hiroyuki Aoki

Department of Biochemistry, Faculty of Science, Okayama University of Science, 1-1 Ridai-cho, Okayama 700, Japan

Abstract

Variation of the thermotropic behaviour of both lipid assemblies and associated water molecules with an increase in water content was investigated for negatively charged phosphatidyl-glycerol (PG)–water system up to 90 wt.% water by DSC. The number of water molecules existing in interbilayer regions of the present gel phase was estimated from a deconvolution analysis of ice-melting DSC curves. On the basis of a result of the calorimetric analysis, a water–distribution diagram was constructed over the water content range from 0 to 90 wt.%. The diagram presented a continuous incorporation of interlamellar water up to 90 wt.% water, related to unilamellar-vesicle forming properties of charged lipids. Furthermore, similarly to a result for neutral lipid systems previously reported by us, the present diagram also showed the existence of a specific water content region (i.e., pre-region) where a structural change of planar to curved bilayers for multilamellar structures proceeds with the aid of bulk-like water before finally reaching unilamellar vesicles.

Keywords: DSC, electron microscopy, interlamellar water, negatively charged phosphatidyl-glycerol

Introduction

There are a great variety of phospholipids in biological membranes. Among these phospholipids, acidic phospholipids, which are negatively charged at neutral pH, have attracted the attention of many investigators, from the viewpoint of their structural and functional role in biomembranes. To date, on the basis of extensive research on charged lipids [1–5], it has been reported that their fundamental bilayer structures are much more sensitive to environmental concentrations of external protons and cations, compared with those of neutral phospholipids such as phosphatidylcholine (PC) and phosphatidyl-ethanolamine (PE). In this connection, we have found that both the mean diameter and the number of bilayers of Na^+-dimyristoylphosphatidylglycerol (DMPG) vesicles (lipid concentration: 2 mmol l^{-1}) increase linearly with an increase in external Na^+ con-

0368–4466/98/ $ 5.00

Akadémiai Kiadó, Budapest
Kluwer Academic Publishers, Dordrecht

centration up to 100 mmol l^{-1} [6, 7]. Furthermore, the DMPG vesicles in the presence of Na^+ at high concentrations have been found to convert into a super-assembly of crystalline cylindrical structure on annealing at a gel phase temperature [8].

Additional remarkable properties of the charged lipids, previously reported by other workers [4, 9–11] are continuous incorporation of interlamellar water between bilayers and formation of unilamellar vesicles in dilute regions, indicating that their bilayer structures are sensitive to variations in water content in the samples. These properties are contrasted with a limited hydration and unchanged multilamellar structures up to dilute regions for neutral lipids. In past research on phosphatidyl-serine (PS) by ^2H-NMR technique [10] it has been reported that all the water added is intercalated between the lamellae up to approximately 75 wt.% water content, beyond which bulk free water appears. On this basis, Hauser *et al.* have reported from their X-ray diffraction [4, 9] and calorimetric data [11] that the appearance of excess free water at around 75 wt.% water is a consequence of the break-up of fully-hydrated multilamellar structures, and above this water content, a gradual conversion of the one-phase (multilamellar structures) to two-phase systems (unilamellar vesicles plus excess water) occurs. In this respect, however, in our previous research on neutral lipids [12, 13] we have reported that before reaching a limiting hydration, there is a specific water content region (pre-region) where bulk-like water is present and with the aid of this water, a certain structural change of planar to curved bilayers in multilamellar structures gradually occurs. Such a structural change is much more expected for charged lipids because it is taken as a process preceding a change of multilamellar to unilamellar vesicles which is not observed for neutral lipids. From this viewpoint, in the present study the variation with increasing water content of the distribution of individual water in different bonding modes was investigated for the Na^+-PG–water system. The number of water molecules was estimated from the ice-melting enthalpy obtained by differential scanning calorimetry (DSC). In this calorimetric estimation, ice-melting DSC curves were deconvoluted into multiple components according to a computer program of a Gaussian curve analysis. The thermal properties of Na^+-PG assemblies were investigated by DSC and structural information was obtained by negative-stain electron microscopy.

Materials and methods

Materials and sample preparation

1,2-dimyristoyl-, and 1,2-palmitoyl-*sn*-glycero-3-[phospho-*rac*-(1-glycerol)] (Na^+-DMPG and Na^+-DPPG) were purchased from Sigma Co. (St. Louis, Missouri) and used without further purification as thin-layer chromatography of these lipids showed a single spot. Na^+-DPPG, which was transferred to the high-pressure crucible cell of a Mettler differential scanning calorimeter (TA-4000,

Switzerland), was dehydrated under high vacuum (10^{-4} Pa) at room temperature for at least 3 days until no mass loss was detected by electroanalysis (Cahn Electrobalance, California). The crucible cell containing the dehydrated Na^+-DPPG was sealed of in a dry box filled with dry N_2 gas and then weighed by a micro balance (Mettler M3, Switzerland). Samples of the Na^+-DPPG-water mixture ranging in water content {(g water)/(g lipid+g water)×100}, from 0 to about 90 wt.% were prepared by successive addition of the desired amounts of water to the same dehydrated compound (approximately 50 mg) by using a microsyringe. Thus, only the weight of water was changed throughout the preparation of a series of samples of different water contents. The water contents were ascertained by weighing the sample and the cell on a microbalance. In order to ensure homogeneous mixing, all the samples were annealed by repeating thermal cycling at temperatures above and below the lipid phase transition up to at least five times, until the same transition peak was attained. After that, the samples were cooled to –80°C for the differential scanning calorimetry (DSC). After the DSC scan, the mass of the sample and the cell were rechecked on the microbalance.

Differential scanning calorimetry

DSC was carried out with a Mettler TA-4000 apparatus by placing the sample in a high-pressure crucible (pressure resistant: 100 kPa cm^{-2}) and heating it from –80°C to temperatures above that of the formation of the liquid crystal phase at a heating rate of 1.0°C min^{-1}. The thermal behaviour of the lipids at high water contents above 90 mass % was measured by a Microcal MC 2 differential scanning calorimeter.

Electron microscopy

Preparations of the lipid assemblies were examined by negative stain electron microscopy. The preparations were prepared below temperatures of 5–10°C as follows: a drop of the dispersion (lipid concentration: ~2 mmol ml^{-1}) was placed on copper grids covered with carbon-coated collodion films, allowed to remain until becoming dry. After that, a 2% solution of sodium phosphotungstate (pH approx. 7) was added and then, the excess solution was drained. The preparation was examined immediately in a JEOL JEM-2000EX electron microscope operated at 200 kV. All operations were performed at around 20°C.

Results

Thermotropic behaviour of Na^+-PG assemblies

Figure 1a shows the typical thermotropic behaviour of the gel–to–liquid crystal phase transition for the Na^+-DPPG–water system of varying water content up to 90 wt.%. With increasing water content up to 45–50 wt.%, the gel–to–liquid

crystal phase transition peak becomes sharper, simultaneously with the growth of the pretransition peak. However, when the water content is beyond 50 wt.%, the gel–to–liquid crystal transition peak begins to broaden, simultaneously with a diminution of the pretransition peak. The broadening continues up to 90 wt.% water content. Similar broadening of the transition peak is observed for the homologous Na^+-DMPG–water system above 50 wt.% water content. Figure 1b shows results for the Na^+-DMPG system ranging in water content from 50 to 99.8 wt.%. In this Figure, two curves at 98.7 and 99.8 wt.% water contents were obtained by a Microcal calorimeter. Thus, the dependence of the temperature and shape of the transition peak on the water content, was observed for Na^+-PG systems up to dilute regions. Such dependence on the water content is not observed for the transition peak of neutral lipid systems of PC and PE, which becomes independent of water content beyond a critical water content [13, 14].

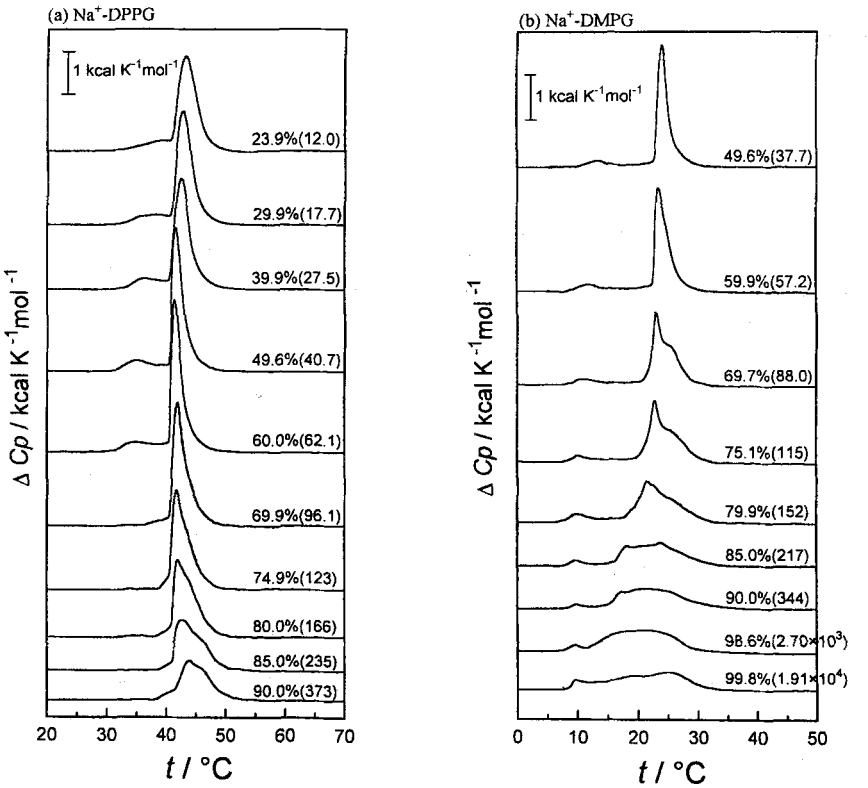

Fig. 1 Thermotropic behaviour of the gel–to–liquid crystal phase transition for Na^+-DPPG–water (a) and Na^+-DMPG–water (b) systems with increasing water content. Apparent, excess heat capacity (ΔC_p) per 1 mol of lipid is plotted as a function of temperature (t). Water content and N_T (=water/lipid molar ratio) are shown at the right-hand-side of each curve. (1 cal corresponds to 4.184 J)

Electron micrographs of Na^+-PG assemblies

Figure 2 shows electron micrographs of Na^+-DMPG (a), DMPC (b) and DMPE (c) assemblies prepared at the same lipid concentration of ~2 mmol l^{-1}). A marked structural difference among these lipid assemblies is the multiplicity of lipid bilayers. Unilamellar vesicles are observed for Na^+-DMPG [6], in contrast to multilamellar structures consisting of regularly stacked lamellae for DMPC [15] and DMPE [16]. However, when the lipid concentration is increased by 10 times for Na^+-DMPG, multilamellar vesicles surrounded by a few lamellae (Fig. 2d) is observed in place of unilamellar vesicles. Comparison of the electron micrographs of Na^+-DMPG in Fig. 2, although limited to two samples of different concentrations, suggests that the multiplicity of bilayers surrounding the vesicles depends on the water content up to dilute regions, similarly to their gel–to–liquid crystal transition peak shown in Fig. 1. On this basis, it is suggested that the broadening of the transition peak for Na^+-PG shown in Fig. 1 results from a change of the vesicles into structures containing fewer layers. By contrast, a fixed transition peak up to dilute regions for the neutral lipids is due to an unchanged multiplicity of their multilamellar structures [11, 14].

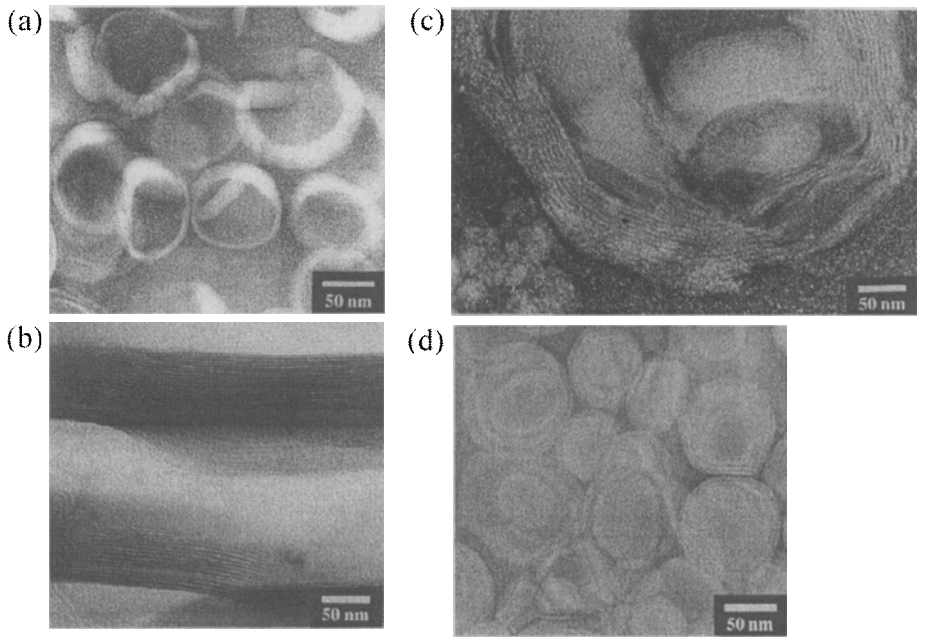

Fig. 2 Negative stain-electron micrographs of lipid assemblies of Na^+-DMPG (a), DMPC (b) and DMPE–water (c) systems prepared at the same lipid concentration of ~2 mmol l^{-1}. The micrograph of Na^+-DMPG assembly prepared at a lipid concentration of ~20 mmol l^{-1} is shown in (d) of this figure

Thermotropic behaviour of water in different bonding modes

Figure 3 shows a series of typical ice-melting DSC curves for the Na^+-DPPG–water system, which appear at temperatures below the gel–to–liquid crystal transition shown in Fig. 1a. Based upon Fig. 3, a variation with water content of the ice-melting behaviour in the present gel phase is outlined as follows. At a water content lower than 8 wt.%, all the water added is not frozen on cooling to –80°C (curve a), showing the existence of nonfreezable water, most likely located in regions between PG head groups in the interbilayer region (nonfreezable interlamellar water). When the water content is increased beyond the critical point of 8 wt.%, an ice-melting peak first appears at low temperatures below 0°C and the peak grows into a broad component extending over a wide temperature range to –45°C with increasing water content (curves b–d). A further increase in water content leads to the appearance of a sharp peak following the broad peak (curve e) and subsequent marked growth of the sharp component (curves f–o). Almost the same ice-melting behaviour as that shown in Fig. 3 has been observed for PC and PE systems of varying water content [12, 13, 17]. On the basis of our previous studies, the broad component is assigned to interlamellar water interacting with the lipid head groups in the interbilayer region. However, the temperature of onset of the sharp components for the present charged lipid system is about 3–4°C lower than that of the corresponding components for the neutral lipid systems. As is well known, a sharp ice-melting peak with the temperature of onset at around 0°C is assigned to bulk free water. Accordingly, the lower temperature of onset of the present sharp component suggests the presence of interlamellar water very close to bulk water in bonding mode. On this basis, it is shown that in the present gel phase, interlamellar water exists, as a whole, in two populations, greatly differing in bonding mode and characterized by the broad and sharp ice-melting components, respectively.

According to the definitions mentioned above, the total number of water molecules added per lipid molecule (N_T) for the present Na^+-DPPG system of varying water content is expressed by the following equation:

$$N_T = N_{I(nf)} + N_{I(f)} + N_B$$

where $N_{I(nf)}$, $N_{I(f)}$ and N_B are the numbers of nonfreezable interlamellar, freezable interlamellar and bulk water molecules per lipid, respectively. If the bulk-like water in the present system is assumed to behave as the so-called free water, N_B is estimated from both the enthalpy change of the sharp component at 0°C for the ice-melting peak and the known melting enthalpy of hexagonal ice, 1.436 kcal mol^{-1}. Subsequently, the total number of (nonfreezable+freezable) interlamellar water molecules, $N_I=N_{I(nf)}+N_{I(f)}$, is also determined from $N_T–N_B$. Following this method, all the ice-melting DSC curves shown in Fig. 3 were deconvoluted according to a computer program ORIGIN (Microcal Software, Inc.) based upon a multiple Gaussian curve analysis. Typical results of the deconvolution analysis are shown in Fig. 4, where the number of deconvoluted curves was

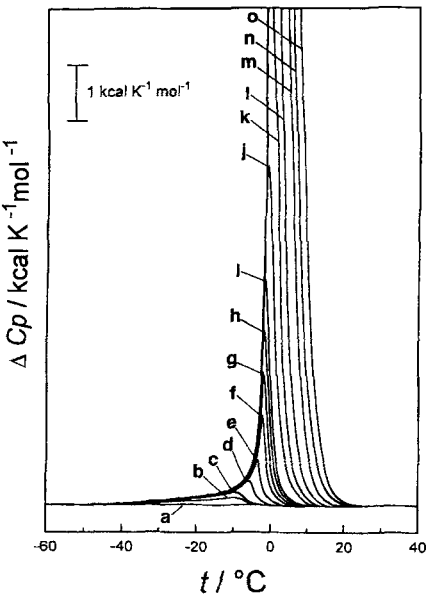

Fig. 3 A series of ice-melting DSC curves for the gel phase of Na^+-DPPG–water system with increasing water content. Apparent excess heat capacity (ΔC_p) per 1 mol of lipid is plotted as a function of temperature (t). Water content (wt.%): (a) 8.1; (b) 11.9; (c) 14.1; (d) 16.0; (e) 18.0; (f) 21.1; (g) 23.9; (h) 27.0; (i) 29.9; (j) 39.9; (k) 49.6; (l) 60.0; (m) 69.9; (n) 74.9; (o) 80.0; (1 cal corresponds to 4.184 J)

made a minimum under the condition that a theoretical curve comparable to the sum of deconvoluted curves is best fitted to the experimental DSC curve. In Fig. 4, resultant deconvoluted curves and a theoretical curve are shown by dotted lines. In Fig. 4a, the broad component of the ice-melting curves is shown to be deconvoluted into three curves I, II and III. Both the half-height width and mid-point temperature of each of these deconvoluted curves were fixed throughout the deconvolutions. With an increase in water content, a newly-deconvoluted curve IV was added, which markedly grows and the deconvoluted curve IV was followed by a deconvoluted curve IV′ (Fig. 4b). Considering the characteristic property of DSC curves that an increase in the amount of sample results in a broadening of the curve at the high-temperature-side, the deconvoluted curves IV and IV′ could be taken as corresponding to either the same component or slightly different ones. Both the deconvoluted curves IV and IV′ continue to grow over the water contents investigated up to 90 wt.%, in contrast to limited growth of the deconvoluted curves I, II and III. At approximately 45 wt.% water content, a deconvoluted curve V with the temperature of onset at around 0°C begins to appear and grows with increasing water content (Fig. 4c). The deconvoluted curve V is also followed by deconvoluted curves V′ and V″ because of the broadening character of the DSC curve (Fig. 4d).

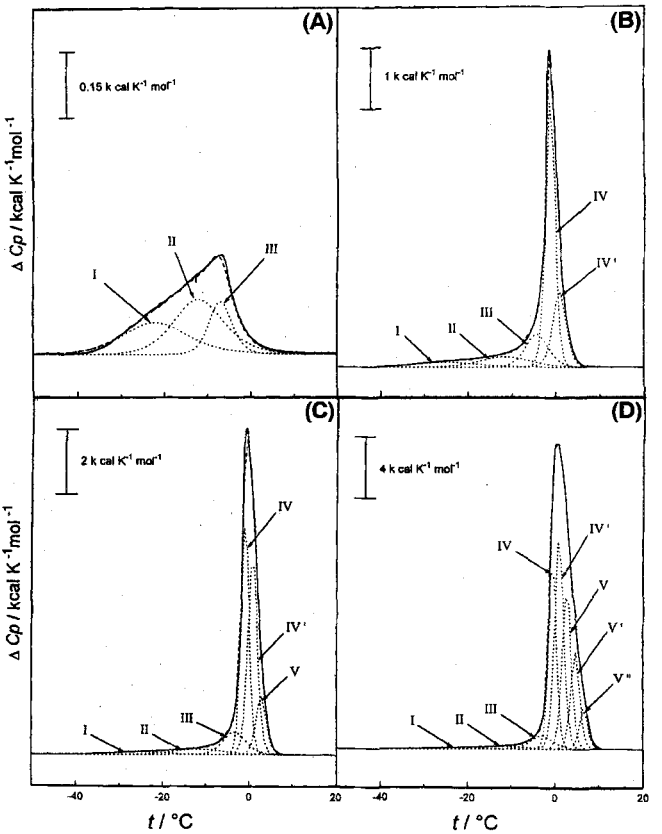

Fig. 4 Deconvolution analyses of ice-melting DSC curves for the gel phases of the Na^+-DPPG–water system at water contents of 14.1 (A), 34.9 (B), 49.6 (C) and 69.9 (D) wt.%. The deconvolutions were performed according to a computer program ORIGIN (Microcal Software, Inc.) based upon a multiple Guassian curve analysis. In each figure, deconvoluted curves and the theoretical curve are shown by dotted lines. The apparent excess heat capacity (ΔC_p) per 1 mol of lipid is plotted as a function of temperature (t). (1 cal corresponds to 4.184 J)

Estimation of the number of individual water molecules in different bonding modes

The enthalpy change, ΔH_5, the sum of individual enthalpy changes of the deconvoluted curves V, V′ and V″ for bulk-like water is plotted as a function of the total number of water molecules per lipid (N_T) in Fig. 5.

In this Figure, the ΔH_5 curve is compared with a theoretical curve ($=1.43_6 N_T$) given by assuming that all the water added is present as free water. The ΔH_5 curve increases gradually over the N_T range from 35 (45 wt.% water) to 125 (75 wt.%

water), after which it increases linearly, but more gently than the theoretical curve does. Thus, the enthalpy difference between the theoretical and ΔH_5 curves, i.e., given by 1.43_6 $N_I(=N_T-N_B)$, becomes larger with increasing water content, indicating that the amount of interlamellar water increases continuously up to N_T=374 (90 wt.%). The behaviour of the ΔH_5 *vs.* N_T curve in Fig. 5 is quite different from that of the corresponding curve for PC–, and PE–water systems previously reported by us [12, 13]. In these neutral lipid systems, the ice-melting enthalpy curve for the bulk water becomes parallel to the theoretical curve above a critical point, at which the amount of the interlamellar water reaches a maximum. This indicates a marked difference between infinite or limited hydrations for the charged and neutral lipids.

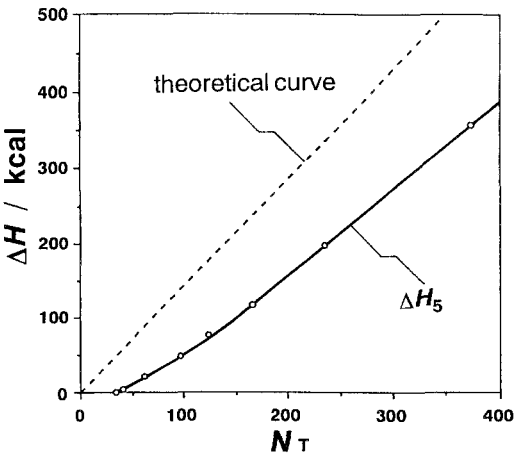

Fig. 5 Variation with increasing water/lipid molar ratio (N_T) of ice-melting enthalpy changes (ΔH_5) per 1 mol of lipid for bulk-like water. The enthalpy curve was obtained by summing up individual enthalpy changes of deconvoluted ice-melting curves V, V′ and V″. The dotted line shows a theoretical curve obtained from the melting enthalpy of hexagonal ice. (1 cal corresponds to 4.184 J)

According to the above-described method, the number of the bulk water molecules (N_B) at each N_T was estimated by dividing an individual value of ΔH_5 by 1.43_6 and furthermore, the number of interlamellar water molecules (N_I) was estimated by subtracting the resultant value of N_B from the value of N_T.

Individual enthalpy changes, ΔH_1, ΔH_2, ΔH_3, ΔH_4 and $\Delta H_4'$, of the deconvoluted curves I, II, III, IV and IV′ for the freezable interlamellar water are plotted against N_T in Fig. 6a. In this Figure the sums of these enthalpy changes, ΔH_T, is also plotted. In Fig. 6a, the continuously increasing behaviour of the sum of the enthalpy curves is shown to result from the ΔH_4 and $\Delta H_4'$ curves which are different from the other three curves saturated at low water contents. Thus, it is revealed that the interlamellar water, which is very close to bulk-like water in

bonding mode, brings about the infinite hydration for the present charged lipid system.

On the other hand, as shown by an enlarged Figure in Fig. 6b, the sum of enthalpy curves intersects the abscissa at approximately N_T=4.0, above which the freezable interlamellar water is obtained. It seems reasonable to consider that lipid hydrocarbon-chains interacting via attractive van der Waals forces limit the amount of water (i.e., nonfreezable interlamellar water) interposed in regions between its head groups. From this viewpoint, 4.0 water molecules per lipid at the intersection point are a limiting value for the nonfreezable interlamellar water in the Na^+-DPPG system. By subtracting the limiting value of $N_{I(nf)}$ from the value of N_I obtained above, the number of freezable interlamellar water molecules $N_{I(f)}$ was estimated for each N_T. In Fig. 7, a cumulative value of $N_{I(nf)}$, $N_{I(f)}$ and N_B is plotted *vs.* N_T.

Discussion

The water–distribution diagram of the Na^+-DPPG–water gel phase in Fig. 7 indicates the following results: (i) all the water added up to N_T=4.0 is present as nonfreezable interlamellar water, most likely existing in regions between the head groups; (ii) all the water added over the N_T range from 4.0 to approximately 35 (water content: 45 wt.%) is present as freezable interlamellar water between the bilayers; and (iii) above N_T=35, some of the water added is present as freezable interlamellar water and the remainder as bulk-like water outside the bilayers.

A noticeable feature in Fig. 7 is the continuous uptake of the freezable interlamellar water up to N_T=374, which is different from the limiting hydration for the neutral lipid systems. In accordance with this difference, in dilute aqueous regions, the present PG system forms unilamellar vesicles, in contrast with multilamellar structures of neutral lipid systems (Fig. 2). Such characteristic proper-

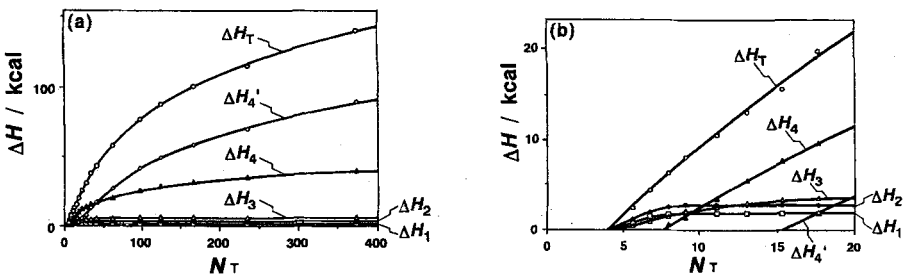

Fig. 6 Variation with increasing water/lipid molar ratio (N_T) of individual ice-melting enthalpy changes (ΔH) per 1 mol of lipid for the freezable interlamellar water, together with the sum of these enthalpy changes. ΔH_1, ΔH_2, ΔH_3, ΔH_4 and $\Delta H_4'$ represent enthalpy changes for deconvoluted ice-melting curves I, II, III, IV and IV', respectively, and ΔH_T shows the sum (a). Fig. 6a at low water contents is shown in an enlarged scale. (1 cal corresponds to 4.184 J) (b)

ties of negatively charged lipids have been reported by Hauser and coworkers throughout a series of studies for PS–water systems [4, 9, 11]. It has been pointed out by them that repulsive forces of the ionic double-layer between opposing bilayers cause the continuous incorporation of interlamellar water, so that multilamellar structures break up and subsequently, closed unilamellar vesicles are reorganized. Furthermore, based upon data of deuteron NMR spectral splittings for PS–^2H_2O liquid crystal phase, Finer *et al.* [10] have reported that all the water added up to 75 wt.% water (N_T=140) is incorporated between the lipid bilayers (20 molecules of bound water plus 120 molecules of trapped free water) and beyond this water content, bulk water appears. When compared with these previous studies [4, 9–11], however, the present study shows some differences, particularly in the water distribution, although the general features of charged lipid–water systems are the same. Therefore the present results are discussed with emphasis on the differences.

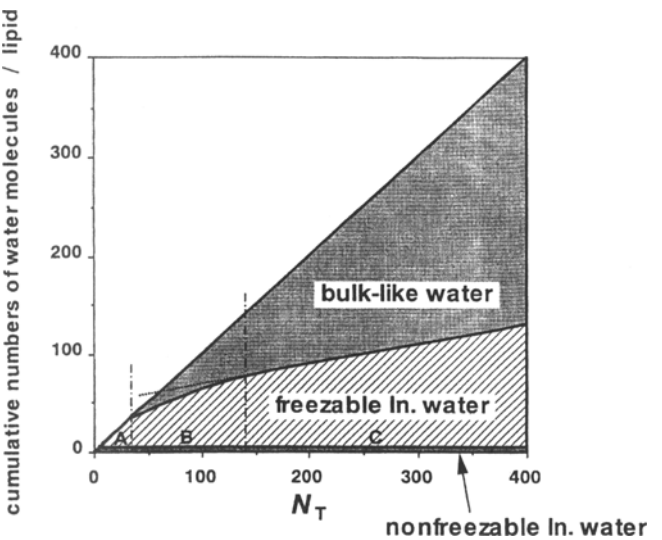

Fig. 7 Variation with increasing water/lipid molar ratio (N_T) of the distribution of nonfreezable and freezable interlamellar water and bulk water. A cumulative number of these water molecules per lipid is plotted against water/lipid molar ratio (N_T). The diagrams are grouped into three categories A (N_T<40), B (40≤N_T≤140) and C (N_T>140). A dotted line is obtained by extrapolating the freezable interlamellar water curve of region C to lower N_T regions

From the diagram of Fig. 7, it becomes apparent that the bulk-like water begins to appear at least at N_T=40 (50 wt.% water). The diagrams are grouped into three categories: A (N_T<40), B (40≤N_T≤140) and C (N_T>140), in which the slope of the freezable interlamellar water curve decreases in this order. Here, particular attention is paid to region B, where the slope of the freezable interlamellar water curve goes down, little by little, with increasing water content up to

N_T=140~150. The existence of such a specific water content region, taken as a pre-region, has been reported in our previous paper [12, 13] for neutral lipid systems; although beyond this water content the freezable interlamellar water curve of these systems becomes parallel to the abscissa because of a limiting hydration. Thus, like neutral lipid systems, the present charged lipid system also shows the existence of the pre-region where the bulk-like water appears at a water content lower than that (N_T=60) expected by an extrapolated line (dotted lines), as shown in Fig. 7. The existence of such a pre-region in lipid–water systems has been previously reported by other workers, mainly from X-ray diffraction studies [18, 19]. In these papers, paying attention to the role of the bulk-like water, it has been proposed that the water in question is located in regions between adjacent vesicles because this water appears simultaneously with a vesiculation of planar multilamellar structure. Therefore, the conversion into multilamellar vesicles for Na^+-DPPG is suggested to occur in region B. In accord with this structural change, a gradual broadening of the gel–to–liquid crystal transition peaks is observed for water contents of region B (Fig. 1a and b). This phenomenon is more clearly recognized in Fig. 8, where the half-height width ($\Delta T_{1/2}$) of gel–to–liquid crystal transition peaks for Na^+-DPPG (a) and Na^+-DMPG (b) is plotted as a function of N_T. In this connection, a broadening of X-ray low-angle diffraction peaks at water contents above 50 wt.% for NH_4^+-DMPS has been reported by Hauser *et al.* [11]. These facts seem to support the present result that similarly to neutral lipids, the vesiculation for negatively charged lipids proceeds in the pre-region with the aid of the bulk-like water. In previous papers published by other workers [4, 9–11], no pre-region is observed for PS systems.

In region C (140~150≤N_T≤374) of the diagram in Fig. 7, the freezable interlamellar water of the present PG system still continues to increase, although slowly, with increasing water content up to N_T=374. However, the amount of interlamellar water, even at water contents as high as N_T=374, is smaller than the limiting value of 140 water molecules/lipid for the PS system estimated by Finer *et al.* [10]. In Fig. 8, a marked broadening of the gel–to–liquid crystal transition peaks is observed for N_T≥140~150, that is, in region C. In this respect, our previous study [6] has revealed that a structural change of unilamellar to multilamellar vesicles for Na^+-DMPG by adding NaCl results in a marked sharpening of the gel–to–liquid crystal transition peak. Additionally, we have reported a similar phenomenon associated with a conversion of DMPC sonicated vesicles into stable multilamellar vesicles on annealing at a gel phase temperature [15]. On this basis, it is most likely that in region C closed multi-bilayers surrounding PG vesicles are broken away successively from the outside with increased water content until finally reaching single lamellar vesicles (Fig. 2a) because the amount of interlamellar water continues to increase up to dilute regions. Such an infinite hydration could be induced by an increased repulsion between opposing PG bilayers, which is a consequence of a lowering in Na^+ concentration in the interbilayer, caused by the increased amount of interlamellar water.

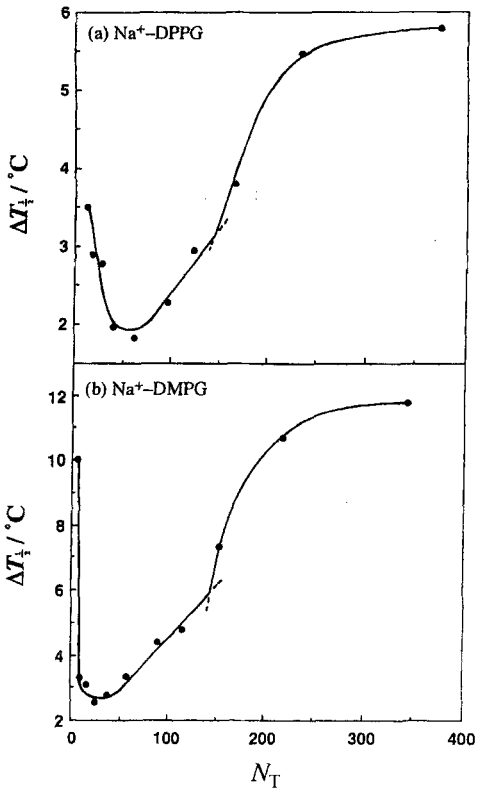

Fig. 8 Variation with increasing water/lipid molar ratio (N_T) of half-height width ($\Delta T_{1/2}$) of gel–to–liquid crystal transition peaks for the Na^+-DPPG (a) and Na^+-DMPG–water (b) systems. The half-height width is plotted against the water/lipid molar ratio (N_T)

Based upon the above-discussed results, the aggregation properties of negatively charged lipids, Na^+-PG can be summarized as follows: (1) for N_T <40, planar multilamellar stacks with increased amount of interlamellar water; (2) for $40 \leq N_T \leq 140$, structural change (vesiculation) from the planar stacks to completely closed multilamellar vesicles with increased amount of both interlamellar water and bulk-like water; and (3) for $N_T \geq 140 \sim 150$, structural change from the multilamellar vesicles to single lamellar vesicles with increased amount of both interlamellar water and bulk-like water.

References

1 A. Watts, K. Harlos and D. Marsh, Biochim. Biophys. Acta, 645 (1981) 91.
2 J. K. Ranck and J. F. Tocanne, FEBS Lett., 143 (1982) 171.
3 J. M. Boggs and G. Rangaraj, Biochemistry, 22 (1983) 5425

4 H. Hauser, Biochim. Biophys. Acta, 772 (1984) 37.
5 D. A. Wilkinson, D. A. Tirrell, A. B. Turek and T. J. McIntosh, Biochim. Biophys. Acta, 905 (1987) 447.
6 M. Kodama and T. Miyata, Thermochim. Acta, 267 (1995) 365.
7 M. Kodama and T. Miyata, Colloid Surfaces A, 109 (1996) 283.
8 M. Kodama, T. Miyata and T. Yokoyama, Biochim. Biophys. Acta, 1168 (1993) 243.
9 9 D. Atkinson, H. Hauser, G. G. Shipley and J. M. Stubbs, Biochim. Biophys. Acta., 339 (1974) 10–29.
10 E. G. Finer and A. Darke, Chem. Phys. Lipids, 12 (1974) 1–16.
11 H. Hauser, F. Paltauf and G. G. Shipley, Biochemistry, 21 (1982) 1061–1067.
12 H. Aoki and M. Kodama, Thermochim. Acta, (in press)
13 M. Kodama, H. Aoki, H. Takahashi and I. Hatta, Biochim. Biophys. Acta, (in press).
14 M. Kodama, M. Kuwabara and S. Seki, Biochim. Biophys. Acta, 689 (1982) 567.
15 M. Kodama, T. Miyata and Y. Takaichi, Biochim. Biophys. Acta, 1169 (1993) 90.
16 M. Kodama, H. Inoue and Y. Tsuchida, Thermochim. Acta, 266 (1995) 373.
17 M. Kodama, Thermochim. Acta, 109 (1983) 81.
18 G. Klose, B. König, H. W. Meyer, G. Schulze and G. Degovics, Chem. Phys. Lipids, 47 (1988) 225.
19 J. F. Nagle, R. Zhang, S. Tristram-Nagle, W. Sun, H. I. Petrache and R. M. Suter, Biophys. J., 70 (1996) 1419.